Temperature dependent complex photonic band structures in two-dimensional photonic crystals composed of high-temperature superconductors

2008 J. Phys.: Condens. Matter 20 275203

(http://iopscience.iop.org/0953-8984/20/27/275203)

J. Phys.: Condens. Matter **20** (2008) 275203 (8pp) doi:10.1088/0953-8984/20/27/275203

Temperature dependent complex photonic band structures in two-dimensional photonic crystals composed of high-temperature superconductors

Chuan Cheng, Can Xu[1], Tao Zhou, Xiao-Fang Zhang and Ying Xu

Key Laboratory for Magnetism and Magnetic Materials of the Ministry of Education, School of Physical Science and Technology, Lanzhou University, Lanzhou Gansu 73000, People's Republic of China

E-mail: cxulzu@yahoo.com

Received 7 January 2008, in final form 13 May 2008
Published 2 June 2008
Online at stacks.iop.org/JPhysCM/20/275203

Abstract

Complex photonic band structures in two-dimensional photonic crystals composed of high-temperature superconductors (HTSCs) for the case of E-polarization are calculated as a function of temperature below T_c, where T_c is the critical temperature of the HTSC. The calculations are based on a temperature dependent complex dielectric function, which includes contributions of both superconducting electrons (SCEs) and normal conducting electrons (NCEs), and a frequency dependent plane wave expansion method. Both temperature independent and temperature dependent damping term in the dielectric function are considered to calculate dispersion relations and the lifetime of the eigenmodes. The results are compared with those obtained by existing calculation methods, which neglect the contribution of NCEs. Our results correspond quite well with those obtained by the existing method in the low-temperature range $0 < T/T_c \leqslant 0.3$; however, results obtained with the two methods are quite different in the temperature range $0.3 < T/T_c \leqslant 1$. We demonstrate that the contribution of NCEs is non-negligible with increasing temperature.

1. Introduction

Photonic crystals, which have spatially periodic dielectric functions, have attracted growing interest in recent years [1–10]. This is mainly because photonic band structures (PBSs) may contain photonic band gaps (PBGs) in which all the electromagnetic (EM) modes are missing. This is an opportunity for us to mold the flow of light for photonic information technology [4]. PBSs strongly depend on the geometry of the lattice and the dielectric indices of the components. Once the geometry is constructed, a possible way to change the PBSs is to change the component materials. Much work has been done to calculate PBSs with different components, such as dielectrics, semiconductors, metals and liquid crystals [5–10].

Recently, photonic crystals composed of superconductors have been studied via the plane wave expansion method [12–15]. Because of the unique optical properties of superconductors, such a system is interesting [15]. A two-fluid model is used to describe the electrodynamics of a superconductor at nonzero temperature [11]. Because plasma frequencies in superconductors are strongly influenced by temperature and the external magnetic field, it is possible to use these properties to realize tunable photonic crystals. Takeda *et al* calculated PBSs of two-dimensional (2D) photonic crystals composed of copper oxide high-temperature superconductors (HTSCs). They found that those photonic crystals exhibited tunability by temperature and external magnetic field [12]. Feng *et al* studied tunable negative refractions in 2D photonic crystals with superconductor components. They found that the refractive angle could be scanned from positive to negative based on the dependence of the superconductor's permittivity on temperature [14]. Pei *et al* proposed a tunable Mach–Zehnder interferometer with a 2D photonic crystal us-

[1] Author to whom any correspondence should be addressed.

ing copper oxide HTSCs. Simulation results showed that light transmission in the photonic crystal Mach–Zehnder interferometer can be modulated from 92.7% to 1.4% with different temperature distributions [13]. The contribution of normal conducting electrons (NCEs) was neglected in these papers in the temperature range below T_c, where T_c is the critical temperature of a superconductor. As a result, the dielectric function of the superconductor was reduced to a simple Drude model [13]. However, as we will show below, the contribution of NCEs cannot be neglected when the temperature increases, especially at temperatures close to T_c.

In this paper, we consider contributions of both superconducting electrons (SCEs) and NCEs. Temperature dependent complex PBSs of 2D periodic systems with copper oxide HTSC components are calculated based on the frequency dependent plane wave expansion method. We only consider the E-polarized EM waves, as in [12–15]. The electric field is parallel to the direction of the cylinders (the z axis) for the 2D photonic crystal structure in the xy plane. Noting that copper oxide HTSCs are highly anisotropic, with in-plane (ab plane) conductivity much larger than that in the c axis [22], where the a, b, c axes are the three principal axes of copper oxide HTSCs. We should clarify that the electric field of the E-polarized EM waves is parallel to the c axis: $E_z \parallel c$. Both temperature independent and temperature dependent damping terms in dielectric function of HTSCs are considered. Temperature dependent PBGs, cut-off frequencies and the lifetime of the eigenmodes are calculated in triangular lattice photonic crystals. Our results are compared with those obtained using the existing calculation method [12, 13], which neglects the contribution of NCEs.

2. Theory

According to the two-fluid model, electrons in the superconductor occupy two states. One is the superconducting state, in which the electrons are paired and transport with no resistance. The other state is the normal state, in which the electrons are not paired and act as NCEs. When the temperature T is lower than the critical temperature T_c of the superconductor, both SCEs and NCEs exist and the sum of their two densities is equal to the total electron density n, which is $n_s + n_n = n$, where n_s and n_n are the densities of SCEs and NCEs, respectively. However, when $T > T_c$, the density of SCEs, n_s, becomes zero and $n_n = n$. In this paper we deal with complex PBSs below T_c.

2.1. Temperature dependent dielectric function of HTSCs

In the two-fluid model we can find the dielectric function $\varepsilon(\omega)$ with respect to order parameter all along the superconductor [12, 16]

$$\varepsilon(\omega) = \varepsilon_\infty \left[1 - \frac{\omega_{sp}^2}{\omega^2} - \frac{\omega_{np}^2}{\omega(\omega + i\gamma)}\right], \tag{1}$$

with

$$\omega_{sp} = \left(\frac{n_s e^2}{m\varepsilon_0\varepsilon_\infty}\right)^{1/2}, \tag{2}$$

$$\omega_{np} = \left(\frac{n_n e^2}{m\varepsilon_0\varepsilon_\infty}\right)^{1/2}, \tag{3}$$

where ω_{sp} and ω_{np} are the plasma frequencies of SCEs and NCEs, respectively. ε_∞ is the dielectric constant of the superconductor and ε_0 is the dielectric constant in a vacuum. $\gamma = \tau^{-1}$ is the damping term of NCEs and τ is the electron relaxation time. e and m are the charge and mass of the electron, respectively. In previous papers, the contribution of NCEs, which is the third term on the right-hand side of equation (1), was neglected [12, 13]. They focused on the microwave or far-infrared region. The damping term γ of their superconductor was much larger than the microwave frequency or far-infrared frequency, thus they said that the contribution of the NCEs could be neglected. But in our calculation we consider the contributions of both SCEs and NCEs. One can see that this contribution is not always small when the temperature increases from 0 K to T_c. We rewrite equation (2) in the form:

$$\omega_{sp} = \frac{c}{\lambda_L(T)\sqrt{\varepsilon_\infty}}, \tag{4}$$

where $c = \frac{1}{\sqrt{\varepsilon_0\mu_0}}$ is the velocity of light in a vacuum and $\lambda_L(T) = (\frac{m}{\mu_0 n_s e^2})^{1/2}$ is the London penetration depth, which is dependent on temperature [17]:

$$\lambda_L(T) = \lambda(0)\left[1 - \left(\frac{T}{T_c}\right)^4\right]^{-1/2}, \tag{5}$$

where $\lambda_L(0)$ is the value of $\lambda_L(T)$ at absolute zero. Substituting equation (5) into equation (4), we have the temperature dependent plasma frequency of SCEs:

$$\omega_{sp} = \frac{c}{\lambda_L(0)\sqrt{\varepsilon_\infty}}\left[1 - \left(\frac{T}{T_c}\right)^4\right]^{1/2}. \tag{6}$$

From equations (2) and (3) we have the relationship between ω_{sp} and ω_{np}, which is $\omega_{np} = \omega_{sp}\sqrt{n_n/n_s}$. Using the Gorter–Casimir result [17]: $n_s/n_n = (T_c/T)^4 - 1$, we obtain the temperature dependent plasma frequency of NCEs:

$$\omega_{np} = \frac{c}{\lambda_L(0)\sqrt{\varepsilon_\infty}}\left(\frac{T}{T_c}\right)^2. \tag{7}$$

As shown in equations (6) and (7), for the condition of $T \leqslant T_c$, the value of ω_{sp} decreases while the value of ω_{np} increases with increasing temperature. Substituting equations (6) and (7) into equation (2), we obtain the temperature dependent dielectric function of HTSCs:

$$\varepsilon(\omega) = \varepsilon_\infty - \frac{c^2}{\lambda_L(0)^2}\left[1 - \left(\frac{T}{T_c}\right)^4\right]\frac{1}{\omega^2} - \frac{c^2}{\lambda_L(0)^2}\left(\frac{T}{T_c}\right)^4\frac{1}{\omega(\omega + i\gamma)}. \tag{8}$$

2.2. Frequency dependent plane wave expansion method

Here we investigate a 2D photonic crystal composed of infinitely long HTSC cylinders. The dielectric constant of the photonic crystal is $\varepsilon(\mathbf{r}_\parallel)$. The periodicity of $\varepsilon(\mathbf{r}_\parallel)$ implies

$$\varepsilon(\mathbf{r}_\parallel + \mathbf{a}_i) = \varepsilon(\mathbf{r}_\parallel) \qquad (i = 1, 2), \tag{9}$$

where $\{\mathbf{a}_i\}$ are the elementary lattice vectors of the 2D photonic crystal and $\mathbf{r}_\parallel$ denotes the 2D position vector (x, y). Because of the spatial periodicity, we can expand $\varepsilon(\mathbf{r}_\parallel)$ in a Fourier series:

$$\varepsilon(\mathbf{r}_\parallel) = \sum_{\mathbf{G}_\parallel} \kappa(\mathbf{G}_\parallel) \exp(\mathrm{i}\mathbf{G}_\parallel \cdot \mathbf{r}_\parallel), \tag{10}$$

where $\mathbf{G}_\parallel = l_1\mathbf{b}_1 + l_2\mathbf{b}_2$ is the reciprocal lattice vector of the 2D photonic crystal. To determine the Fourier coefficients $\{\kappa(\mathbf{G}_\parallel)\}$ of $\varepsilon(\mathbf{r}_\parallel)$, whose cross section is a circle of radius r_a, in the particular case of cylinders characterized by the dielectric function, we write $\varepsilon(\mathbf{r}_\parallel)$ in the form

$$\varepsilon(\mathbf{r}_\parallel) = \varepsilon_\mathrm{b} + [\varepsilon(\omega) - \varepsilon_\mathrm{b}]\, S(\mathbf{r}_\parallel), \tag{11}$$

with

$$S(\mathbf{r}_\parallel) = \begin{cases} 1 & \text{for } |\mathbf{r}_\parallel| \leqslant r_\mathrm{a}, \\ 0 & \text{for } |\mathbf{r}_\parallel| > r_\mathrm{a}, \end{cases} \tag{12}$$

where ε_b is the dielectric constant of the background dielectric material in which the HTSC cylinders are embedded. Here we deal with frequency independent background dielectric materials. The inverse Fourier transform gives

$$\kappa(\mathbf{G}_\parallel) = \varepsilon_\mathrm{b}\delta_{\mathbf{G}_\parallel 0} + [\varepsilon(\omega) - \varepsilon_\mathrm{b}]\frac{1}{a_\mathrm{c}}\int_{a_\mathrm{c}} \mathrm{d}\mathbf{r}_\parallel S(\mathbf{r}_\parallel)\exp(-\mathrm{i}\mathbf{G}_\parallel \cdot \mathbf{r}_\parallel)$$
$$= \varepsilon_\mathrm{b} + [\varepsilon(\omega) - \varepsilon_\mathrm{b}]\, f, \qquad \text{for } \mathbf{G}_\parallel = 0 \tag{13}$$

$$\kappa(\mathbf{G}_\parallel) = \varepsilon_\mathrm{b}\delta_{\mathbf{G}_\parallel 0} + [\varepsilon(\omega) - \varepsilon_\mathrm{b}]\frac{1}{a_\mathrm{c}}\int_{a_\mathrm{c}} \mathrm{d}\mathbf{r}_\parallel S(\mathbf{r}_\parallel)\exp(-\mathrm{i}\mathbf{G}_\parallel \cdot \mathbf{r}_\parallel)$$
$$= [\varepsilon(\omega) - \varepsilon_\mathrm{b}]\, f\frac{2J_1(G_\parallel r_\mathrm{a})}{G_\parallel r_\mathrm{a}}, \qquad \text{for } \mathbf{G}_\parallel \neq 0 \tag{14}$$

where $a_\mathrm{c} = |\mathbf{a}_1 \times \mathbf{a}_2|$ is the area of the unit cell, $f = \pi r_\mathrm{a}^2/a_\mathrm{c}$ is the fill fraction and $J_1(x)$ is a Bessel function. As a matter of convenience, we first substitute equation (1) into equations (13) and (14), and then replace ω_sp and ω_np by the right-hand side of equations (6) and (7), respectively, in numerical calculation. From equations (1), (13) and (14), we obtain

$$\kappa(\mathbf{G}_\parallel) = (1-f)\varepsilon_\mathrm{b} + f\varepsilon_\infty\left[1 - \frac{\omega_\mathrm{sp}^2}{\omega^2} - \frac{\omega_\mathrm{np}^2}{\omega(\omega + \mathrm{i}\gamma)}\right], \quad \text{for } \mathbf{G}_\parallel = 0 \tag{15}$$

$$\kappa(\mathbf{G}_\parallel) = \left\{\varepsilon_\infty\left[1 - \frac{\omega_\mathrm{sp}^2}{\omega^2} - \frac{\omega_\mathrm{np}^2}{\omega(\omega + \mathrm{i}\gamma)}\right] - \varepsilon_\mathrm{b}\right\} f\frac{2J_1(G_\parallel r_\mathrm{a})}{G_\parallel r_\mathrm{a}}, \quad \text{for } \mathbf{G}_\parallel \neq 0. \tag{16}$$

In the case of E-polarization, the nonzero components of the electric field $\mathbf{E}(\mathbf{r}_\parallel; t)$ and the magnetic field $\mathbf{H}(\mathbf{r}_\parallel; t)$ are

$$\mathbf{E}(\mathbf{r}_\parallel; t) = [0, 0, E_z(\mathbf{r}_\parallel)]\exp(-\mathrm{i}\omega t), \tag{17}$$

$$\mathbf{H}(\mathbf{r}_\parallel; t) = [H_x(\mathbf{r}_\parallel), H_y(\mathbf{r}_\parallel), 0]\exp(-\mathrm{i}\omega t). \tag{18}$$

$H_x(\mathbf{r}_\parallel)$ and $H_y(\mathbf{r}_\parallel)$ can be expressed in terms of $E_z(\mathbf{r}_\parallel)$, and the Maxwell equation for the electric field is reduced to

$$\left(\frac{\partial^2}{\partial x^2} + \frac{\partial^2}{\partial y^2}\right)E_z(\mathbf{r}_\parallel) + \varepsilon(\mathbf{r}_\parallel)\frac{\omega^2}{c^2}E_z(\mathbf{r}_\parallel) = 0. \tag{19}$$

To solve this equation we expand $E_z(\mathbf{r}_\parallel)$ according to

$$E_z(\mathbf{r}_\parallel) = \sum_{\mathbf{G}_\parallel} A(\mathbf{G}_\parallel)\exp\left[\mathrm{i}(\mathbf{k}_\parallel + \mathbf{G}_\parallel)\cdot\mathbf{r}_\parallel\right], \tag{20}$$

where $\mathbf{k}_\parallel$ is the wavevector in the first Brillouin zone. From equations (10), (19) and (20), we have the following eigenvalue equation for the expansion coefficients [18]:

$$(\mathbf{k}_\parallel + \mathbf{G}_\parallel)^2 A(\mathbf{G}_\parallel) = \frac{\omega^2}{c^2}\sum_{\mathbf{G}'_\parallel}\kappa(\mathbf{G}_\parallel - \mathbf{G}'_\parallel)A(\mathbf{G}'_\parallel)$$
$$= \frac{\omega^2}{c^2}\kappa(0)A(\mathbf{G}_\parallel) + \frac{\omega^2}{c^2}{\sum_{\mathbf{G}_\parallel}}'\kappa(\mathbf{G}_\parallel - \mathbf{G}'_\parallel)A(\mathbf{G}'_\parallel), \tag{21}$$

where the prime on the sum over $\mathbf{G}'_\parallel$ indicates that the term with $\mathbf{G}'_\parallel = \mathbf{G}_\parallel$ is omitted. Substituting equations (15) and (16) into equation (21), and replacing ω_sp and ω_np by the right-hand side of equations (6) and (7) we obtain

$$\left[\left(\frac{\omega}{c}\right)^3\mathbf{B} + \left(\frac{\omega}{c}\right)^2\mathbf{C} + \frac{\omega}{c}\mathbf{D} + \mathbf{M}\right]\mathbf{A} = 0, \tag{22}$$

where $\mathbf{A}$ is the column vector of $\{A(\mathbf{G}_\parallel)\}$; $\mathbf{B}$, $\mathbf{C}$, $\mathbf{D}$ and $\mathbf{M}$ are $NG \times NG$ matrices, and NG is the number of plane waves employed in the expansions of $\varepsilon(\mathbf{r}_\parallel)$ and $E_z(\mathbf{r}_\parallel)$. The elements of the matrices are given by

$$\mathbf{B}_{\mathbf{G}_\parallel,\mathbf{G}'_\parallel} = \left[\varepsilon_\mathrm{b} + (\varepsilon_\infty - \varepsilon_\mathrm{b})f\right]\delta_{\mathbf{G}_\parallel,\mathbf{G}'_\parallel} + (\varepsilon_\infty - \varepsilon_\mathrm{b})f\frac{2J_1(|G_\parallel - G'_\parallel|r_\mathrm{a})}{|G_\parallel - G'_\parallel|r_\mathrm{a}}, \tag{23}$$

$$\mathbf{C}_{\mathbf{G}_\parallel,\mathbf{G}'_\parallel} = \mathrm{i}\frac{\gamma}{c}\left[\varepsilon_\mathrm{b} + (\varepsilon_\infty - \varepsilon_\mathrm{b})f\right]\delta_{\mathbf{G}_\parallel,\mathbf{G}'_\parallel} + \mathrm{i}\frac{\gamma}{c}(\varepsilon_\infty - \varepsilon_\mathrm{b})f\frac{2J_1(|G_\parallel - G'_\parallel|r_\mathrm{a})}{|G_\parallel - G'_\parallel|r_\mathrm{a}}, \tag{24}$$

$$\mathbf{D}_{\mathbf{G}_\parallel,\mathbf{G}'_\parallel} = -\left[\frac{f}{\lambda_\mathrm{L}(0)^2} + (\mathbf{k}_\parallel + \mathbf{G}_\parallel)^2\right]\delta_{\mathbf{G}_\parallel,\mathbf{G}'_\parallel} - \frac{f}{\lambda_\mathrm{L}(0)^2}\frac{2J_1(|G_\parallel - G'_\parallel|r_\mathrm{a})}{|G_\parallel - G'_\parallel|r_\mathrm{a}}, \tag{25}$$

$$\mathbf{M}_{\mathbf{G}_\parallel,\mathbf{G}'_\parallel} = -\mathrm{i}\frac{\gamma}{c}\left\{\frac{f}{\lambda_\mathrm{L}(0)^2}\left[1 - \left(\frac{T}{T_\mathrm{c}}\right)^4\right] + (\mathbf{k}_\parallel + \mathbf{G}_\parallel)^2\right\}\times\delta_{\mathbf{G}_\parallel,\mathbf{G}'_\parallel} - \mathrm{i}\frac{\gamma}{c}\frac{f}{\lambda_\mathrm{L}(0)^2}\left[1 - \left(\frac{T}{T_\mathrm{c}}\right)^4\right]\frac{2J_1(|G_\parallel - G'_\parallel|r_\mathrm{a})}{|G_\parallel - G'_\parallel|r_\mathrm{a}}. \tag{26}$$

Equation (22) is a nonlinear problem of the third order, which can be reformulated as a linear problem in $3NG$ dimensions [3, 19]. We rewrite equation (22) in this form:

$$\left(-\beta^2\mathbf{B}^{-1}\mathbf{C} - \beta\mathbf{B}^{-1}\mathbf{D} - \mathbf{B}^{-1}\mathbf{M}\right)\mathbf{A} = \beta^3\mathbf{A}, \tag{27}$$

where $\beta = \omega/c$. Here equation (27) is reformulated as a matrix of order $3NG \times 3NG$

$$\begin{pmatrix} \mathbf{0} & \mathbf{I} & \mathbf{0} \\ \mathbf{0} & \mathbf{0} & \mathbf{I} \\ -\mathbf{B}^{-1}\mathbf{M} & -\mathbf{B}^{-1}\mathbf{D} & -\mathbf{B}^{-1}\mathbf{C} \end{pmatrix}\begin{pmatrix} \mathbf{A} \\ \beta\mathbf{A} \\ \beta^2\mathbf{A} \end{pmatrix} = \beta\begin{pmatrix} \mathbf{A} \\ \beta\mathbf{A} \\ \beta^2\mathbf{A} \end{pmatrix}, \tag{28}$$

where $\mathbf{I}$ is a $NG \times NG$ identity matrix. The complete solution of equation (22) is obtained by solving for the eigenvalues of equation (28). We write the eigenvalues, which are complex, in the form

$$\beta = \frac{\omega_\mathrm{R}}{c} + \mathrm{i}\frac{\omega_\mathrm{I}}{c}, \tag{29}$$

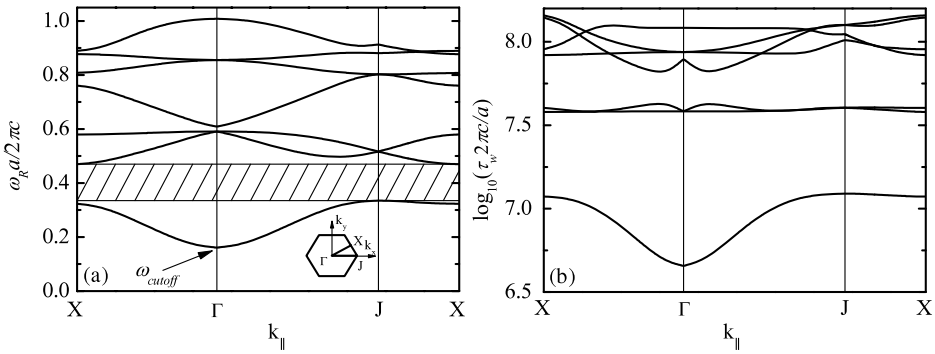

Figure 1. Complex photonic band structure of the two-dimensional photonic crystal composed of high-temperature superconductor ($Bi_{1.85}Pb_{0.35}Sr_2Ca_2Cu_{3.1}O_y$) cylinders at $T = 5$ K. (a) The real part of complex photonic band structure; (b) the imaginary part of complex photonic band structure: the lifetime of the lowest seven eigenmodes associated with the real part of complex photonic band structure shown in (a). $\varepsilon_\infty = 12$, $\varepsilon_b = 1$, $r_a = 0.2a$, $\gamma = 1$ THz, $NG = 1585$.

where ω_R represents the real part of the frequency and ω_I determines the lifetime τ_w of the eigenmodes associated with the PBSs, according to the definition [3]

$$\frac{1}{\tau_w} = -2\omega_I. \tag{30}$$

Since the eigenvalues are the general solutions of the eigenequation (28), we have to discarded the solutions which correspond to unphysical modes, i.e. those with a negative real part ω_R/c and with a positive imaginary part ω_I/c yielding a negative lifetime.

3. Numerical calculation and discussion

In the calculation there is another important problem we should consider: is the damping term $\gamma = \tau^{-1}$ temperature dependent or temperature independent? In this section, we first use a fixed damping term to calculate the temperature dependent PBSs and the lifetime of the eigenmodes associated with the PBSs. The results obtained by our method are compared with those obtained by the approximation method [12, 13], which neglects the contribution of NCEs. Both methods use the same parameters. Then we use a temperature dependent damping term following an exponential relation, which has been detected in experiments [20, 21], to calculate the temperature dependent PBSs and the lifetime of the eigenmodes. The exponential relation will be discussed in detail in section 3.2. And the results are also compared with those obtained by the method in [12, 13].

3.1. Using a fixed damping term while T/T_c changes from 0 to 1

We utilize infinitely long cylinders of the copper oxide HTSC $Bi_{1.85}Pb_{0.35}Sr_2Ca_2Cu_{3.1}O_y$ to form a 2D photonic crystal with a triangular lattice. In previous papers [12, 13], PBSs of this crystal have been investigated using the approximation method which neglects the contribution of NCEs. Here we use the same initial parameters in [13] in order to compare our results with those obtained in that paper. The initial parameters are: the critical temperature is $T_c = 107$ K; the dielectric constant of the HTSC is $\varepsilon_\infty = 12$; the background of the photonic crystal is air ($\varepsilon_b = 1$); the lattice constant is $a = 100$ μm; the radius of the cylinder is $r_a = 0.2a$; at 5 K, the London penetration depth is $\lambda_L(5) = 23$ μm, and the London penetration depth at absolute zero, $\lambda_L(0)$, can be obtained from equation (5), which is $\lambda_L(0) = 1.45 \times a/2\pi$ (the London penetration depth is normalized in units of $a/2\pi$). We assume that the damping term of this HTSC is relatively weakly temperature dependent, so we suppose that it is fixed with increasing temperature, and is $\gamma = 1$ THz. In calculation, the damping term is normalized in units of $2\pi c/a$, which is $\gamma = 5.31 \times 10^{-2} \times 2\pi c/a$. In figure 1(a), we plot the real part of the PBS for E-polarized EM waves propagating through the 2D triangular lattice at $T = 5$ K. As shown in this figure, the cut-off frequency is the lowest frequency. In other words, there is no eigenmode which has a smaller frequency than that. Figure 1(b) is the lifetime of the lowest seven eigenmodes associated with PBS shown in figure 1(a). A total of 1585 plane waves were used to obtain these results.

As shown in figure 1(a), a PBG exists in the range from $0.335 \times 2\pi c/a$ to $0.470 \times 2\pi c/a$ (the ordinate plots frequencies in lattice units of $2\pi c/a$). This gap range is almost the same as the result obtained in [13] (using the same parameters), which is from $0.33 \times 2\pi c/a$ to $0.47 \times 2\pi c/a$. This means that at low temperatures ($T \ll T_c$) the contribution of the NCEs can be neglected, because the results obtained by the two methods—neglecting and not neglecting this contribution—are almost the same. In fact, we can guess from equation (8). From this equation, the contribution of NCEs, which is the third term on the right-hand side of equation (8), is directly proportional to $(T/T_c)^4$. Thus when $T \ll T_c$, the contribution of NCES is quite small, so it can be neglected and has little influence on the result of PBS. However, the contribution of NCEs increases by four orders of magnitude with increasing temperature. When T/T_c approaches 1, this contribution cannot be neglected, as shown below.

In order to investigate the influence of neglecting the contribution of NCEs and not neglecting this contribution, we calculate the dependence of the midgap ω_{mid} (the frequency at the middle of a PBG) and the PBG per midgap ratio $\Delta\omega_R/\omega_{mid}$ on temperature of this photonic crystal and compare our results

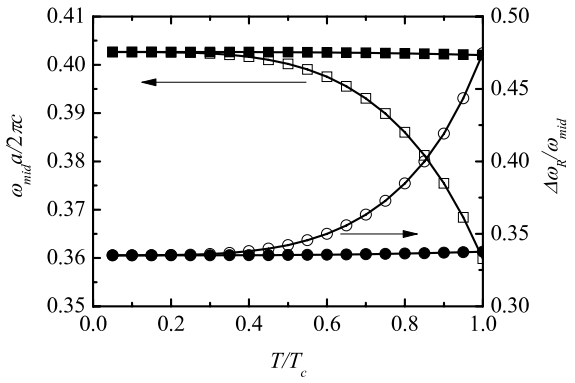

Figure 2. Dependence of the midgap (square symbols) and the photonic band gap per midgap ratio (circle symbols) on temperature. Solid symbols indicate the results obtained with our method which considers the contribution of NCEs. Hollow symbols indicate the results obtained by the method [12, 13], which neglects the contribution of NCEs. $\varepsilon_\infty = 12$, $\varepsilon_b = 1$, $r_a = 0.2a$, $\gamma = 1$ THz, $NG = 618$.

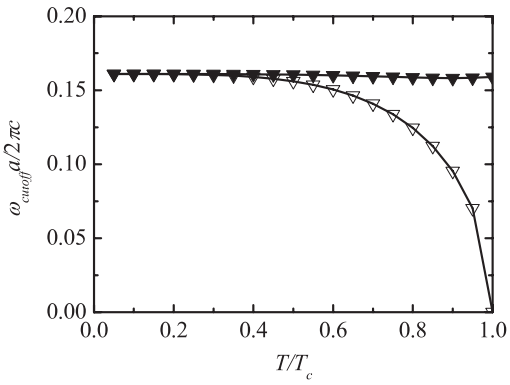

Figure 3. Dependence of the cut-off frequency on temperature. Solid symbols indicate the results obtained with our method which considers the contribution of NCEs. Hollow symbols indicate the results obtained by the method [12, 13], which neglects the contribution of NCEs. $\varepsilon_\infty = 12$, $\varepsilon_b = 1$, $r_a = 0.2a$, $\gamma = 1$ THz, $NG = 618$.

with those obtained by the method used in [12, 13]. We have found that the convergence of these calculations is rapid and a relatively small number of plane waves is required to obtain an accurate PBS for the case of E-polarization, so a total of 618 plane waves are used to obtain the results for all values of T/T_c and an error of the eigenvalues for 618 plane waves is less than 0.1% in comparison to results obtained using 1585 plane waves. We focus on a PBG which appears between the first and the second photonic bands, as shown in figure 1(a).

In figure 2, ω_{mid} and $\Delta\omega_R/\omega_{mid}$ are plotted as a function of temperature. The results were obtained by our method which considers the contribution of NCEs and the method in [12, 13] which neglects that contribution. For the results obtained with our method, both ω_{mid} and $\Delta\omega_R/\omega_{mid}$ change a little with increasing temperature, actually they almost on a horizontal line. On the other hand, for the results obtained by the method in [12, 13], ω_{mid} decreases monotonically while $\Delta\omega_R/\omega_{mid}$ increases monotonically with increasing temperature, which is similar to [12], although we use different parameters from them in this calculation. In figure 2, the localization of ω_{mid} and the value of $\Delta\omega_R/\omega_{mid}$ obtained by both methods are almost the same in the low-temperature range $0 < T/T_c \leqslant 0.3$; however, after T/T_c exceeds 0.3, the difference between the results becomes larger and larger with increasing temperature, which means that the contribution of the NCEs becomes larger. So we come to the conclusion that the contribution of NCEs is non-negligible in the temperature range $0.3 < T/T_c \leqslant 1$. We can comprehend this phenomenon as follows. According to equations (6)–(8), when the temperature increases, the contribution of SCEs decreases by four orders of magnitude of T/T_c, while the contribution of NCEs increases at the same speed. When $T \ll T_c$, the contribution of the NCEs has quite a small influence on the PBSs, so that it can be neglected. However, at temperatures close to T_c, the contribution of the NCEs is far larger than the contribution of the SCEs. If the contribution of the NCEs is neglected (as in [12, 13]), it will have a strong influence on the PBS, resulting in large tunability by temperature as shown in figure 2 (the hollow symbols). But this large tunability does not occur. The reason is that, from equations (6)–(8), if we take contributions of both SCEs and NCEs into consideration, the sum of them changes a little with increasing temperature, which means the dielectric function changes a little, so that the PBS is not greatly changed. That is why ω_{mid} and $\Delta\omega_R/\omega_{mid}$ obtained by our method are almost on a horizontal line. From the comparison of the two methods, the contribution of the NCEs becomes large with increasing temperature and it is non-negligible.

Figure 3 shows the dependence of the cut-off frequency ω_{cutoff} on temperature of this photonic crystal. The results obtained by our method are also compared with those obtained with the existing method [12, 13], which neglects the contribution of NCEs. From figure 3, the difference between the cut-off frequencies obtained by the two methods becomes large with increasing temperature, which is similar to the PBG results shown in figure 2. Especially at $T/T_c = 1$, the cut-off frequency obtained by the method in [12, 13] has disappeared (becomes zero), while the cut-off frequency obtained with our method changes a little. We comprehend this phenomenon at $T/T_c = 1$ as follows. The contribution of SCEs becomes zero at that temperature (the plasma frequency of SCEs $\omega_{sp} = 0$ from equation (6)) while the contribution of NCEs reaches its maximum value (in the temperature range below T_c). For the method in [12, 13], the dielectric function reduces to a constant ε_∞, which is similar to photonic crystals composed of frequency independent dielectric materials which have no cut-off frequency [5]. On the other hand, for our method, the reduced contribution of SCEs is remedied by the contribution of NCEs, so the dielectric function changes a little and the cut-off frequency is not greatly changed, as shown in figure 3 (solid symbols).

We have also calculated PBSs of a 2D photonic crystal with HTSC components in a different lattice (square lattice), which is not shown here. The results are similar to those in figures 2 and 3. Here we conclude that for HTSCs having a relatively weaker temperature dependent damping term (using a fixed damping term in the calculation), PBSs are insensitive

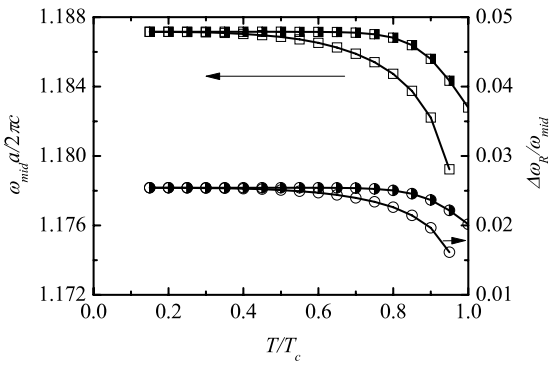

Figure 4. Dependence of the midgap (square symbols) and the photonic band gap per midgap ratio (circle symbols) on temperature. Half-solid symbols indicate the results obtained with our method which considers the contribution of NCEs. Hollow symbols indicate the results obtained with the method in [12, 13], which neglects the contribution of NCEs. $\varepsilon_\infty = 15$, $\varepsilon_b = 1$, $r_a = 0.2a$, $\gamma = p\exp(T/T_1)$, $p = 2.5 \times 10^{10}$ Hz, $T_1 = 0.13T_c$, $NG = 618$.

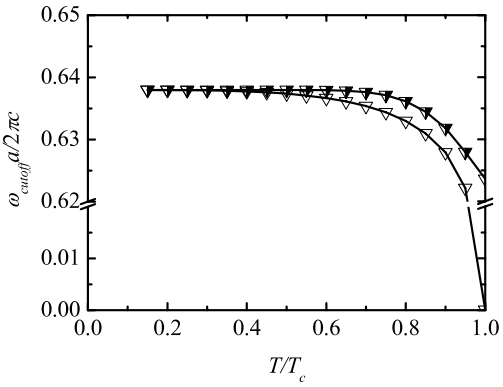

Figure 5. Dependence of the cut-off frequency on temperature. Half-solid symbols indicate the results obtained with our method which considers the contribution of NCEs. Hollow symbols indicate the results obtained by the method in [12, 13], which neglects the contribution of NCEs. $\varepsilon_\infty = 15$, $\varepsilon_b = 1$, $r_a = 0.2a$, $\gamma = p\exp(T/T_1)$, $p = 2.5 \times 10^{10}$ Hz, $T_1 = 0.13T_c$, $NG = 618$.

to increasing temperature in our method. And the contribution of NCEs can be neglected in the low temperature range, which is $0 < T/T_c \leqslant 0.3$ (in our calculation), but in the temperature range $0.3 < T/T_c \leqslant 1$ that contribution is non-negligible.

3.2. Using a temperature dependent damping term while T/T_c changes from 0.15 to 1

We should note that the damping term γ is fixed with increasing temperature in section 3.1. However, there are wide variations in the temperature dependence of the damping term: in materials doped with Zn or Ni or in most thin films, γ is extrinsic and has a relatively weaker temperature dependence; on the other hand, in high-purity single crystals of $YBa_2Cu_3O_{6+x}$, γ falls to microwave frequencies (≈30 GHz) for $T \leqslant 40$ K [23]. Bonn *et al* noted that γ in $YBa_2Cu_3O_{6.95}$ ($T_c = 92.7$ K) follows an exponential law, $\gamma \propto \exp(T/T_0)$, where $T_0 \approx 12$ K, for T between 15 and 84 K [21]. Barrett *et al* noted that all measurements of γ, denoted $W_{1\alpha}$ ($\alpha = a, b, c$ for magnetic fields applied along the three principal axes of the crystal $YBa_2Cu_3O_7$), followed the same exponential behavior, $W_{1\alpha}/T \propto \exp(T/T_0)$, with similar values of T_0 [20, 21]. Thus in this paper we consider a situation in which the HTSC components have a temperature dependent damping term.

In this section, we investigate a 2D photonic crystal composed of infinitely long HTSC cylinders in a triangular lattice. E-polarized EM waves propagate through the photonic crystal. We suppose that the dielectric constant of the HTSC is $\varepsilon_\infty = 15$; the background of the photonic crystal is air ($\varepsilon_b = 1$); the lattice constant is $a = 100$ μm; the radius of the cylinder is $r_a = 0.2a$; the London penetration depth at absolute zero is $\lambda_L(0) = 200$ nm (referring to [15]), which is $\lambda_L(0) = 1.26 \times 10^{-2} \times a/2\pi$. The damping term of the HTSC is temperature dependent, which follows an exponential relation $\gamma = p\exp(T/T_1)$, where $p = 2.50 \times 10^{10}$ Hz ($p = 1.33 \times 10^{-3} \times 2\pi c/a$), $T_1 = 0.13T_c$, for T between $0.15T_c$ and T_c (referring to [21]). Here, the values of p and T_1 are not precise, because we just want to consider a situation with a temperature dependent damping term having an exponential relation which has been detected in experiments [20, 21]. Our results are also compared with those obtained with the existing method [12, 13], which neglects the contribution of NCEs. The number of plane waves used in these calculation is $NG = 618$ for all values of T/T_c. An error of the eigenvalues for 618 plane waves is less than 0.1% in comparison to results obtained using 1585 plane waves.

First, we focus our attention on a PBG which appears in the frequency range $(1.1–1.2)2\pi c/a$. Figure 4 shows the dependence of the midgap ω_{mid} and the PBG per midgap ratio $\Delta\omega_R/\omega_{mid}$ obtained by our method and the method in [12, 13]. From figure 4, ω_{mid} and $\Delta\omega_R/\omega_{mid}$ obtained by the two methods decrease monotonically with increasing temperature. We can see that in the low-temperature range $0.15 \leqslant T/T_c \leqslant 0.3$ the results obtained with the two methods are almost the same. But ω_{mid} and $\Delta\omega_R/\omega_{mid}$ decrease rapidly with increasing temperature for the method in [12, 13], while those values decrease more slowly for our method. Neglecting or not neglecting the contribution of NCEs, different results are obtained in the temperature range $0.3 < T/T_c \leqslant 1$, so the contribution is non-negligible in this temperature range. The cut-off frequency of this photonic crystal has the similar tendency with increasing temperature, as shown in figure 5.

Figure 5 shows the cut-off frequency of this photonic crystal as a function of temperature. Cut-off frequencies obtained by the two methods decrease monotonically with increasing temperature. Moreover, results obtained with our method change more slowly than the results obtained with the method in [12, 13]. Especially at the temperature $T = T_c$, the cut-off frequency obtained by the method in [12, 13] becomes zero (the reason for this has been discussed in section 3.1), while that value obtained with our method is $0.624 \times 2\pi c/a$.

In fact, we can comprehend these results (figures 4 and 5) qualitatively from equations (6)–(8). At a low temperature which is far from T_c, the contribution of the NCEs is in direct proportion to $(T/T_c)^4$, which is quite small, so it can be neglected and has little influence on the eigenvalues. That

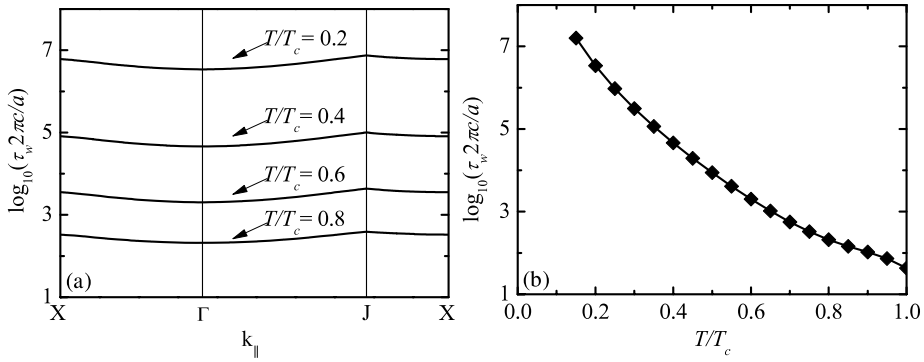

Figure 6. The lifetime of the lowest eigenmode associated with photonic band structure. (a) The lifetime of the lowest eigenmode at $T/T_c = 0.2$, 0.4, 0.6 and 0.8, respectively. (b) The lifetime of the lowest eigenmode at the Γ point as a function of temperature. $\varepsilon_\infty = 15$, $\varepsilon_b = 1$, $r_a = 0.2a$, $\gamma = p\exp(T/T_1)$, $p = 2.5 \times 10^{10}$ Hz, $T_1 = 0.13T_c$, $NG = 618$.

is why the results obtained using the two methods are almost the same in the low-temperature range. But the contribution of SCEs decreases with increasing temperature, while the contribution of NCEs increases. If the contribution of NCEs is neglected as in [12, 13], it will has a large influence on the calculation results in the high-temperature range. That is why the results obtained by the method in [12, 13] change a lot with increasing temperature. In our method, contributions of both SCEs and NCEs are considered; furthermore, the damping term is temperature dependent and increases exponentially with increasing temperature. The contribution of the damping term counteracts some part of the contribution from the NCEs. According to equation (8), by analyzing the Drude formula, an increasing γ counteracts the plasma frequency in the real part of the permittivity. Thus the tendency of the results is the same as that obtained with the method in [12, 13], but changes slowly. Above all, for HTSCs having a temperature dependent damping term, the contribution of the NCEs can be neglected in the low-temperature range, which is $0 < T/T_c \leqslant 0.3$ (in our calculation), but in the temperature range $0.3 < T/T_c \leqslant 1$ that contribution is non-negligible.

The dependence of the lifetime of the lowest eigenmode associated with PBS on temperature has also been investigated for this photonic crystal. In figure 6(a), we plot the lifetime of the lowest eigenmode at different temperatures: $T/T_c = 0.2$, 0.4, 0.6 and 0.8. As shown in figure 6(a), the shape of the lifetime curve is almost unchanged at different temperatures, and the curve just shifts downward with increasing temperature. Figure 6(b) shows the lifetime of the lowest eigenmode at the Γ point as a function of temperature. The lifetime decreases logarithmically with increasing temperature. This shows that the influence of temperature on the lifetime of eigenmodes is greater than the influence on PBSs.

4. Conclusions

We have demonstrated temperature dependent complex PBSs in 2D photonic crystals composed of HTSCs for E-polarized electromagnetic waves propagating in triangular lattices. When using a temperature independent damping term γ, the midgap, the PBG per midgap ratio and the cut-off frequency are insensitive to temperature; our results are different from those obtained with the existing method [12, 13], which show large tunability. However, according to our calculation, large tunability does not occur when we take the contribution of NCEs into consideration. When using a temperature dependent damping term, our results decrease more slowly than those obtained with the existing method. Also, in this condition, the lifetime of the lowest eigenmodes decreases logarithmically with increasing temperature. In both conditions, our results correspond quite well with those obtained using the existing method [12, 13] in the low-temperature range $0 < T/T_c \leqslant 0.3$; however, those two group of results are different in the temperature range $0.3 < T/T_c \leqslant 1$. We include the contribution of NCEs in our calculation, while the method in [12, 13] did not, so our method is more accurate. Therefore, the contribution of NCEs is non-negligible with increasing temperature, especially when T is close to T_c. Our method is suitable for the calculation of temperature dependent complex PBSs composed of HTSCs below T_c.

Acknowledgment

We acknowledge the Open Project of the Key Laboratory for Magnetism and Magnetic Materials of the Ministry of Education, Lanzhou University.

References

[1] John S 1987 *Phys. Rev. Lett.* **58** 2486
[2] Yablonovitch E 1987 *Phys. Rev. Lett.* **58** 2059
[3] Kuzmiak V and Maradudin A A 1997 *Phys. Rev.* B **55** 7427
[4] Bauer J and John J 2007 *Appl. Phys. Lett.* **90** 261111
[5] Plihal M and Maradudin A A 1991 *Phys. Rev.* B **44** 8565
[6] Xu C, Hu X, Li Y, Liu X, Fu R and Zi J 2003 *Phys. Rev.* B **68** 193201
[7] Moreno E, Erni D and Hafner C 2002 *Phys. Rev.* B **65** 155120
[8] Yoshino K, Shimoda Y, Kawagishi Y, Nakayama K and Ozaki M 1999 *Appl. Phys. Lett.* **75** 932
[9] Takeda H and Yoshino K 2004 *Phys. Rev.* E **70** 026601
[10] Gottardo S, Burresi M, Geobaldo F, Pallavidino L, Giorgis F and Wiersma D S 2006 *Phys. Rev.* E **74** 040702(R)

[11] Tinkham M 1996 *Introduction to Superconductivity* 2nd edn (New York: McGraw-Hill)
[12] Takeda H and Yoshino K 2003 *Phys. Rev.* B **67** 245109
[13] Pei T H and Huang Y T 2007 *J. Appl. Phys.* **101** 084502
[14] Feng L, Liu X P, Ren J, Tang Y F, Chen Y B, Chen Y F and Zhu Y Y 2005 *J. Appl. Phys.* **97** 073104
[15] Berman O L, Lozovik Y E, Eiderman S L and Coalson R D 2006 *Phys. Rev.* B **74** 092505
[16] Matsuda Y, Gaifullin M B, Kumagai K, Kadowaki K and Mochiku T 1995 *Phys. Rev. Lett.* **75** 4512
[17] Ooi C H R, Yeung T C A, Kam C H and Lim T K 2000 *Phys. Rev.* B **61** 5920
[18] Kuzmiak V, Maradudin A A and Pincemin F 1994 *Phys. Rev.* B **50** 16835
[19] Brand S, Abram R A and Kaliteevski M A 2007 *Phys. Rev.* B **75** 035102
[20] Barrett S E, Martindale J A, Durand D J, Pennington C H, Slichter C P, Friedmann T A, Rice J P and Ginsberg D M 1991 *Phys. Rev. Lett.* **66** 108
[21] Bonn D A *et al* 1993 *Phys. Rev.* B **47** 11314
[22] Lee W M, Hui P M and Strond D 1995 *Phys. Rev.* B **51** 8634
[23] Schrieffer R J 2007 *Handbook of High-Temperature Superconductivity* (New York: Springer) p 149